The Application of Clinical Genetics

Dovepress
Taylor & Francis Group

Open Access Full Text Article

CASE REPORT

Functional Validation of a Novel Deep Intronic *IMPG2* Variant Causing Pseudoexon Activation in Retinitis Pigmentosa with Macular Involvement

Guobing Zheng[1,*], Chenxia Xu[1,*], Fenghua Xie[1], Qiaoli Li[2], Zhanhui Ou[3], Degang Wang[1], Haijun Li[1]

[1]Prenatal Diagnosis Center, Boai Hospital of Zhongshan, Zhongshan, Guangdong, 528400, People's Republic of China; [2]Department of Ophthalmology, The Sixth Affiliated Hospital of South China University of Technology, Foshan, Guangdong, 528200, People's Republic of China; [3]Reproductive Medicine Center, Boai Hospital of Zhongshan, Zhongshan, Guangdong, 528400, People's Republic of China

*These authors contributed equally to this work

Correspondence: Haijun Li, Prenatal Diagnosis Center, Boai Hospital of Zhongshan, No. 6 Chenggui Road, Zhongshan, Guangdong, 528400, People's Republic of China, Tel +86-076088776370, Email navy1003@163.com

Objective: Retinitis pigmentosa (RP) is a genetically heterogeneous group of inherited retinal dystrophies often accompanied by macular involvement. Variants in *IMPG2* are known to cause RP type 56 and vitelliform macular dystrophy type 5, but the pathogenic role of deep intronic variants has rarely been characterized. This study aimed to identify and functionally validate a novel deep intronic *IMPG2* variant in a patient with RP.

Methods: A comprehensive clinical, genetic, and functional assessment was performed. Ophthalmic evaluations included fundus photography, optical coherence tomography (OCT), OCT angiography (OCTA), and multifocal electroretinography (mfERG). Whole-genome sequencing followed by Sanger validation and segregation analysis was conducted. In silico splicing prediction and dual minigene assays (pcMINI and pcMINI-C) in HEK293T and HeLa cells were employed to evaluate the splicing effect of the variant.

Results: A novel homozygous deep intronic variant in *IMPG2* (NM_016247.4:c.909-1659A>G), absent from public databases, was identified. Splice prediction tools suggested creation of a cryptic donor site. Functional assays demonstrated aberrant splicing with retention of a 132 bp pseudoexon, introducing a premature termination codon and thereby likely triggering nonsense-mediated decay rather than generating a stable truncated protein. Segregation analysis confirmed autosomal recessive inheritance. The proband exhibited lifelong night blindness, progressive peripheral visual field constriction, and macular structural and functional impairment, consistent with *IMPG2*-associated retinopathy.

Conclusion: This study provides the first functional evidence that a deep intronic *IMPG2* variant causes pseudoexon activation leading to a premature termination codon and likely nonsense-mediated decay. These findings expand the *IMPG2* mutational spectrum, highlight the pathogenic potential of deep intronic variants, and emphasize the importance of functional assays for reclassifying variants of uncertain significance in inherited retinal diseases.

Keywords: retinitis pigmentosa, macular involvement, *IMPG2*, deep intronic variant, pseudoexon activation, functional validation

Background

Inherited retinal dystrophies (IRDs) are a group of genetically heterogeneous disorders characterized by the progressive degeneration of retinal photoreceptors or retinal pigment epithelium (RPE). Clinically, IRDs typically present with night blindness, peripheral visual field loss, and progressive decline in visual acuity, which may ultimately lead to blindness.[1,2] Among them, retinitis pigmentosa (RP) is the most common subtype, with a global prevalence estimated at 1 in 3000 to 1 in 5000 individuals. To date, more than 100 genes have been identified as being associated with RP, reflecting its considerable clinical and genetic heterogeneity.[3,4]

https://doi.org/10.2147/TACG.S573156
Received: 18 October 2025
Accepted: 31 December 2025
Published: 22 January 2026

The IMPG2 (interphotoreceptor matrix proteoglycan 2) gene encodes a structural protein localized to the interphotoreceptor matrix between photoreceptors and the RPE, playing a crucial role in maintaining photoreceptor integrity and function. Biallelic variants in IMPG2 have been reported to cause autosomal recessive RP as well as certain subtypes of vitelliform macular dystrophy.[5,6] Patients with IMPG2-related retinopathy often present with bilateral night blindness, progressive peripheral visual field constriction, and characteristic bone-spicule pigmentation in the retina. Optical coherence tomography (OCT) commonly reveals disorganization of the macular architecture, and electrophysiological tests indicate severely impaired retinal function.

Despite major advances in gene discovery, 52–74% of IRD cases remain without a molecular diagnosis after exome- or panel-based testing.[7,8] This "missing heritability" is frequently attributed to pathogenic variants outside coding regions, including deep intronic and regulatory changes.[9] Notably, an estimated 9–30% of pathogenic variants in Mendelian disease act by altering splicing rather than directly changing protein sequence.[9] Whole-genome sequencing (WGS) helps bridge this gap by detecting intronic and structural variants overlooked by whole-exome sequencing (WES), with reported incremental diagnostic yields ranging from a few percentage points to ~24%, depending on cohort and methodology.[10] As deep intronic and structural variants are often missed by WES, WGS has become an essential tool to improve diagnostic yield in IRDs with negative or inconclusive exome results.[10,11] Recent ACMG/ClinGen Splicing Variant Interpretation (SVI) recommendations also emphasize that RNA-based functional assays provide important evidence for interpreting splicing variants, particularly those located in noncanonical or deep intronic regions.[12] Emerging long-read cDNA/RNA sequencing technologies also provide a direct means to detect aberrant splicing events, including pseudoexon activation, and are increasingly applied in IRD diagnostics.[13]

Here, we report a non-consanguineous patient with bilateral night blindness who, by WGS, was found to harbor a novel homozygous deep intronic variant in *IMPG2* (c.909-1659A>G). Using family-based segregation, in silico splice prediction, detailed retinal imaging and electrophysiology, and an in vitro minigene splicing assay, we demonstrate aberrant splicing attributable to this variant. In accordance with ACMG/AMP criteria,[14] the variant was reclassified from VUS to likely pathogenic. These findings expand the *IMPG2* mutational spectrum and highlight the critical role of functional assays in interpreting deep intronic variants in IRDs.

Materials and Methods

Patient and Clinical Evaluation

We enrolled a 54-year-old female proband clinically diagnosed with retinitis pigmentosa (RP). The patient exhibited congenital night blindness, progressive peripheral visual field constriction, and gradual decline in visual acuity in recent years. Comprehensive ophthalmic assessments included medical history review, best-corrected visual acuity measurement, slit-lamp biomicroscopy, fundus photography, optical coherence tomography (OCT), OCT angiography (OCTA), multifocal electroretinography (mfERG), and microperimetry (MAIA).

This study was approved by the Ethics Committee of Boai Hospital of Zhongshan (Approval No.: KY-2025-008-05). Institutional approval was required and obtained for both the study procedures and the publication of the case details. Written informed consent was obtained from all participants in accordance with the Declaration of Helsinki.

Genetic Testing and Bioinformatic Analysis

Genomic DNA was extracted from peripheral blood using EDTA anticoagulation. Whole-genome sequencing (WGS) was performed on the BGI high-throughput platform using paired-end short-read sequencing, with an average depth of 58.95× and >98% of the genome covered at ≥10× (hg19/GRCh37 reference). Variants were analyzed using BGI's standard clinical WGS pipeline, and genes with established disease associations listed in the OMIM database were assessed. Population databases used for variant interpretation included gnomAD (r2.1.1; accessed 20 March 2024), ExAC (r1), 1000 Genomes (Phase 3), and ESP6500 (V2). Disease databases included ClinVar (accessed 20 March 2024) and the BGI-Phoenix internal disease-variant database. HGMD Professional 2024.1 (accessed 20 March 2024) was additionally queried to confirm the absence of previously reported pathogenic variants at this locus. Candidate variants were validated by Sanger sequencing. In silico splicing predictions were generated using SpliceAI, MaxEntScan, and

NNSplice. SpliceAI (version 1.3.1) was applied using a Δ score threshold of ≥0.20 for potential splice-altering effects. Segregation analysis was performed in available family members after written informed consent.

Minigene Splicing Assay

To assess the functional consequences of the intronic variant, minigene constructs were generated using both pcMINI and pcMINI-C vectors. Each construct contained *IMPG2* exons 9 and 10 with the intervening intronic sequence carrying either the wild-type (WT) or mutant (Mut; c.909-1659A>G) allele. Detailed primer sequences used for amplification and cloning are provided in Supplementary Table 1. Additional details of the minigene construction strategy are provided in the Supplementary Methods. Recombinant plasmids were transiently transfected into HEK293T and HeLa cells using a liposome-based method. After 24–48 hours, total RNA was extracted and reverse-transcribed into cDNA. RT-PCR was performed with vector-specific primers, and the products were separated by agarose gel electrophoresis, purified, and sequenced by Sanger sequencing. All experiments were independently repeated at least three times in both cell lines to confirm reproducibility. The design and maps of pcMINI and pcMINI-C constructs are provided in Supplementary Figure 1.

Variant Interpretation and Pathogenicity Assessment

Variant classification was performed according to the ACMG/AMP 2015 guidelines and subsequent refinements.[12,14] Evidence categories included population frequency, computational predictions, segregation analysis, and functional assay results. The final pathogenicity classification was determined based on the integrated evidence.

Results

Clinical Phenotype and Ocular Imaging Findings

The patient exhibited progressive visual decline over the years. Fundus examination revealed widespread bone-spicule-like pigment deposits in the mid-peripheral retina, markedly attenuated retinal vessels, optic nerve atrophy, and waxy pallor of the optic discs.

In October 2019, ophthalmic examinations showed:

a. Microperimetry (MAIA): Poor fixation response in both eyes; central fixation in the left eye was unstable; macular sensitivity was markedly reduced, falling below the 5th percentile reference range.
b. Multifocal electroretinography (mfERG): Residual responses were limited to the central foveal region, with severe peripheral dysfunction.
c. Ultra-widefield fundus imaging (Figure 1A and C): Bone-spicule pigmentation in the mid-periphery, narrowed vessels, and waxy optic discs.
d. OCT (Figure 1B and D): Spectral-domain OCT revealed thinning of the outer retinal layers with generalized loss of the ellipsoid zone in both eyes.
e. OCTA: Demonstrated reduced capillary density in the superficial and deep capillary plexuses.

Clinically, the proband exhibited night blindness from childhood, progressive decline in visual acuity beginning in her 40s, and no improvement in vision following cataract surgery. During the past decade, peripheral visual fields progressively constricted, resulting in increasing difficulty with reading.

Best-corrected visual acuity recorded in 2013 was 0.2 in the right eye (OD) and 0.1 in the left eye (OS). During follow-up, a formal refraction in 2019 showed that best-corrected visual acuity (BCVA) measurement had declined to counting fingers at 20 cm in the right eye, while the left eye remained partially correctable to 0.3−, indicating preserved but progressively impaired central visual function. A summary of the longitudinal clinical findings is provided in Table 1.

Peripheral blood samples were obtained from available family members, including the proband, her parents, three siblings, her husband, and her two children, following informed consent. Sanger sequencing was conducted to evaluate

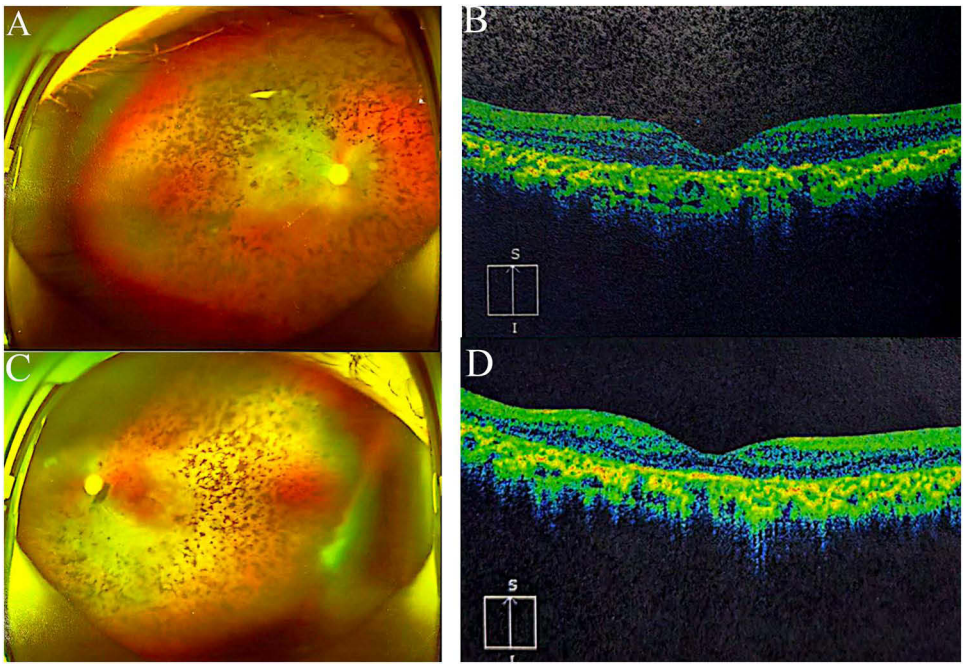

Figure 1 Ocular imaging findings of the proband. (**A** and **C**) Ultra-widefield fundus images obtained using the Optos Daytona P200T scanning laser ophthalmoscope (Optos PLC, Dunfermline, UK), showing scattered bone-spicule–like pigment deposits in the mid-peripheral retina, attenuated retinal vessels, optic nerve pallor, and waxy discs. (**B** and **D**) Spectral-domain optical coherence tomography (SD-OCT) images acquired using the Cirrus HD-OCT 5000 system (Carl Zeiss Meditec, Dublin, CA, USA) with the Macular Cube 512×128 protocol, demonstrating thinning of the outer retinal layers and generalized loss of the ellipsoid zone in both eyes.

co-segregation of the identified variant with the disease phenotype, and a pedigree diagram was generated to illustrate the inheritance pattern.

Genetic Testing Results

Whole-genome sequencing identified a novel homozygous deep intronic variant in the *IMPG2* gene (NM_016247.4: c.909-1659A>G), located between exons 9 and 10, approximately 1659 bp from the exon–intron boundary. Genome-wide runs of homozygosity analysis from the clinical WGS data showed no large homozygous segments. This variant was absent from gnomAD, ClinVar, HGMD, and dbSNP. Sanger sequencing was performed in nine relatives, including

Table 1 Clinical Timeline Summarizing Major Symptoms, BCVA, Functional Tests, and Imaging Findings

Year	Symptoms	BCVA (OD/OS)	Functional Tests	Imaging Findings
Childhood	Night blindness; peripheral blurring	–	–	–
2013	Central vision preserved	0.2 / 0.1	–	Fundus/OCT: RP with macular involvement
2018	Peripheral field severely restricted	Not recorded	–	OCT: CST 271 μm; EZ loss RNFL: OD 117 μm, OS 108 μm Fundus: bone-spicules
2019	Central blurring (OD > OS)	OD: CF/20 cm; OS: 0.3−	MAIA: reduced sensitivity; unstable fixation mfERG: only central island preserved	–
2023	Further decline in daily visual function	Not recorded	Uncorrected VA: HM/50 cm IOP: 12–13 mmHg	OCT: CST 193 μm RNFL: OD 98 μm OCTA: reduced capillary density Fundus image: classic RP pattern

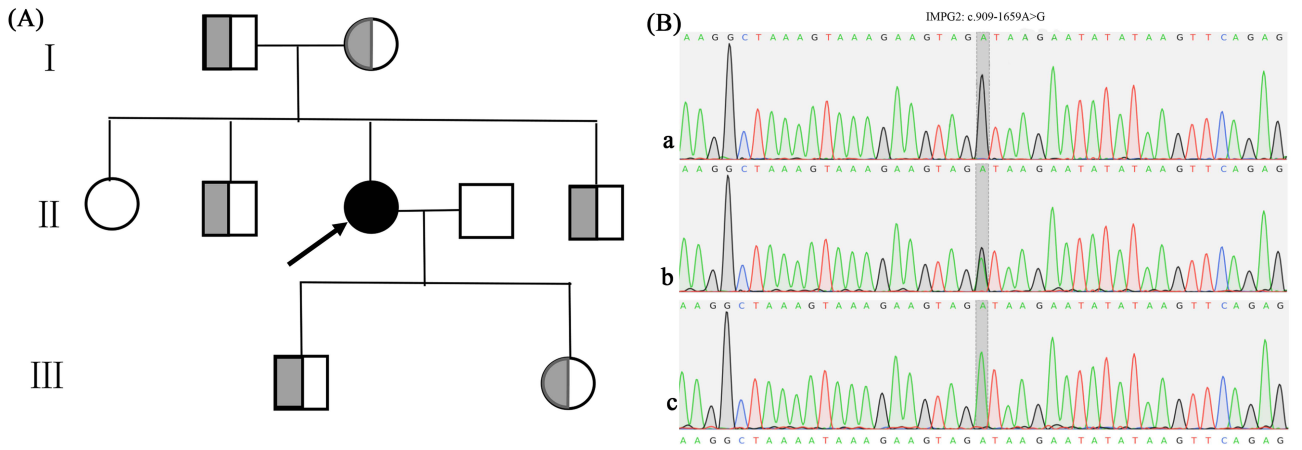

Figure 2 Pedigree and Sanger sequencing validation of the IMPG2 c.909-1659A>G variant. (**A**) Pedigree of the family showing the segregation of the variant; the proband (arrow) is homozygous, and all tested relatives were confirmed by Sanger sequencing. (**B**) Sanger sequencing chromatograms. (a) homozygous mutant (proband); (b) heterozygous carrier; (c) wild-type individual.

the proband, her parents, three siblings, her husband, and her two children. Segregation analysis demonstrated that both parents were heterozygous carriers, consistent with autosomal recessive inheritance, whereas unaffected siblings carried either the heterozygous or wild-type allele (Figure 2).

Bioinformatic Prediction and Minigene Splicing Assay Results

In silico analysis predicted a deleterious effect of the *IMPG2* c.909-1659A>G variant. SpliceAI yielded a score of 0.55, exceeding the recommended 0.50 threshold for a strong predicted splicing impact. Consistently, both MaxEntScan and NNSplice indicated impaired recognition of the native splice site and activation of a cryptic donor site, supporting the likelihood of pseudoexon inclusion.

To experimentally validate these predictions, dual minigene constructs (pcMINI and pcMINI-C) carrying either the wild-type (WT) or mutant (Mut) sequence were transfected into HEK293T and HeLa cells (Figure 3A). In all four experimental systems (pcMINI-HEK293T, pcMINI-HeLa, pcMINI-C-HEK293T, pcMINI-C-HeLa), RT-PCR revealed that WT constructs generated a single band of the expected size, whereas Mut constructs consistently produced an aberrant band with altered mobility (Figure 3B; original uncropped gels shown in Supplementary Figure 2). Splicing diagrams illustrated canonical exon 9–10 junctions in WT transcripts, while Mut transcripts showed retention of a 132 bp pseudoexon, introducing a premature termination codon (PTC) (Figure 3C). Sanger sequencing further confirmed pseudoexon retention in Mut transcripts (Figure 3D).

Collectively, these results demonstrate that the *IMPG2* c.909-1659A>G variant induces a robust and reproducible splicing defect across different vector and cell systems. The aberrant inclusion of a 132 bp pseudoexon introduces a PTC, making nonsense-mediated decay the most likely outcome and reducing the likelihood of generating a stable truncated protein.

Variant Pathogenicity Assessment

Based on the ACMG/AMP guidelines, the *IMPG2* c.909-1659A>G variant was evaluated for pathogenicity. Its extremely low allele frequency in population databases such as gnomAD and dbSNP provided supporting evidence of rarity (PM2_Supporting). Segregation analysis demonstrated that both parents were heterozygous carriers, consistent with autosomal recessive inheritance, providing additional supporting evidence (PM3_Supporting). Functional validation using dual minigene splicing assays revealed a reproducible splicing defect with pseudoexon retention and generation of a premature termination codon, meeting the PVS1_Moderate criterion. In addition, the proband's clinical presentation—typical of IMPG2-related retinal dystrophy—provided phenotype specificity supporting PP4. Taken together, these criteria support the classification of the *IMPG2* c.909-1659A>G variant as Likely pathogenic (Table 2). The final ACMG/AMP evidence codes applied were PVS1_Moderate, PM2_Supporting, PM3_Supporting, and PP4, in accordance with the ClinGen SVI framework.[12,14]

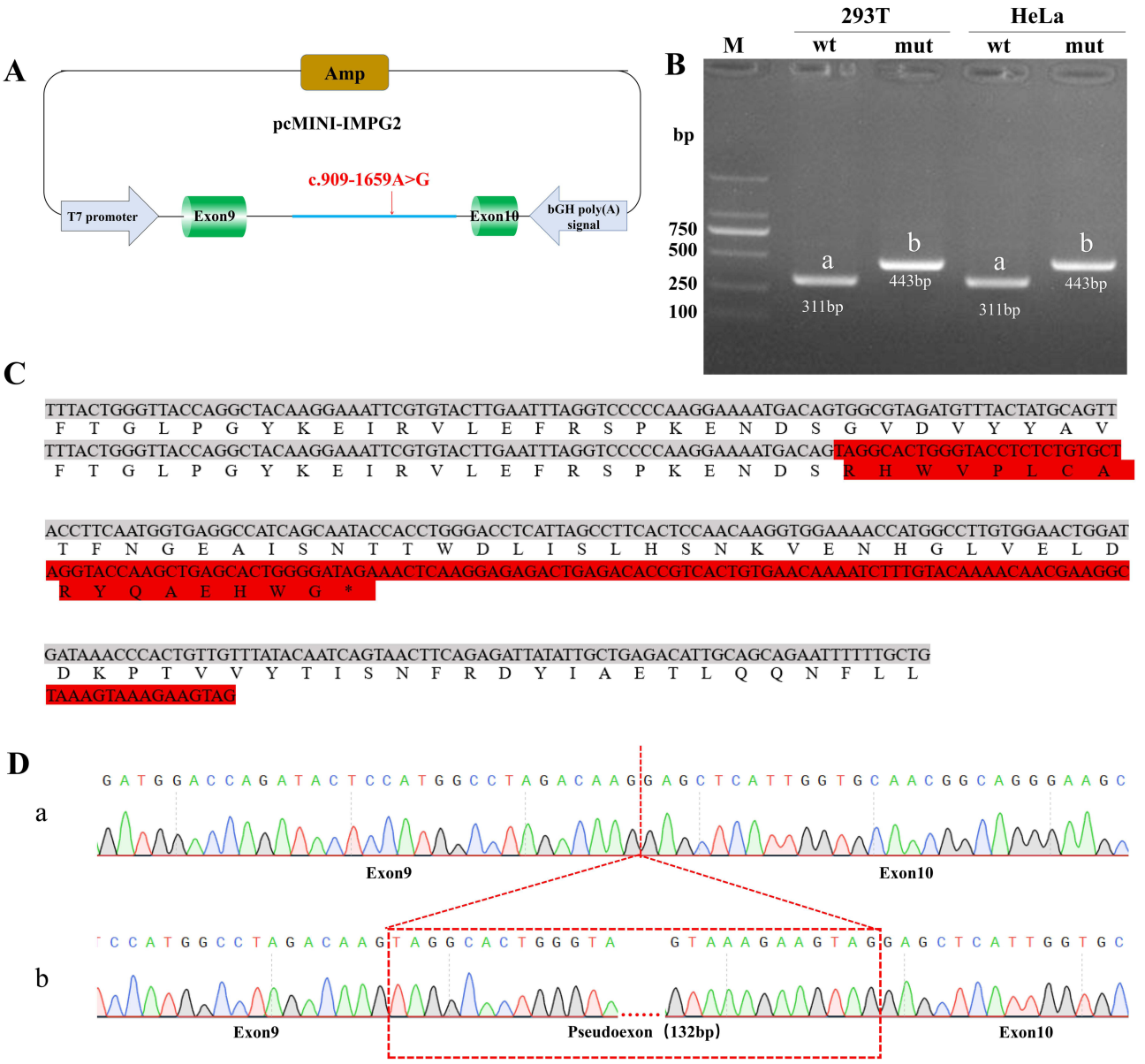

Figure 3 Minigene splicing assay of the *IMPG2* c.909-1659A>G variant (pcMINI system). (**A**) Schematic of the pcMINI-IMPG2 constructs. (**B**) RT-PCR products from HEK293T and HeLa cells. Expected sizes: 311 bp (WT) and 443 bp (Mut, with 132-bp pseudoexon inclusion); observed bands matched these predictions. (**C**) Splicing patterns of WT and Mut transcripts; the red segment represents the 132-bp pseudoexon activated by the variant, which introduces a premature stop codon. (**D**) Sanger sequencing confirming the exon9–pseudoexon–exon10 junction in the Mut transcript.

Discussion

This study reports, for the first time, a functionally validated deep intronic variant of *IMPG2* (c.909-1659A>G) associated with retinitis pigmentosa (RP) and macular involvement. *IMPG2* is a known causative gene, with biallelic variants leading to autosomal recessive RP (RP56), and both monoallelic and biallelic variants implicated in vitelliform macular dystrophy.[15] Previous studies have demonstrated that pathogenic *IMPG2* variants are predominantly located in exons or canonical splice sites, with a substantial proportion resulting in truncated proteins.[5,16,17] In contrast, the variant identified in this study activates a cryptic splice site, leading to retention of a 132 bp pseudoexon and the introduction of a premature termination codon. Because the premature termination codon lies upstream of the final exon–exon junction, nonsense-mediated decay is highly likely, and heterologous minigene assays cannot fully recapitulate endogenous retinal

https://doi.org/10.2147/TACG.S573156

Table 2 Summary of the IMPG2 c.909-1659A>G Variant and ACMG Classification

Chromosomal Location (GRCh37/hg19)	Transcript (NM Number)	Gene	Nucleotide Change	Zygosity	Source	Evidence code	ACMG Classification	Intron	Phenotype (OMIM)
chr3:100978276	NM_016247.4	*IMPG2*	c.909-1659A>G	Homozygous	Parental	PVS1_Moderate PM2_Supporting PM3_Supporting PP4	Likely pathogenic	Intron 9	Retinitis pigmentosa 56 (OMIM:613581)/AR Macular dystrophy, vitelliform, 5 (OMIM:616152)/AD

https://doi.org/10.2147/TACG.S573156

nonsense-mediated decay efficiency. This expands the mutational spectrum of *IMPG2* and highlights the pathogenic potential of deep intronic variants, which are often overlooked in routine genetic testing.

The clinical features of our proband—including lifelong night blindness, progressive visual decline, peripheral visual field constriction, and macular dysfunction—are consistent with previously described phenotypes of *IMPG2*-associated retinopathy.[5,15,16] Importantly, while earlier reports indicated that macular involvement is common and often occurs early in *IMPG2*-related RP, our findings further demonstrate that a noncoding deep intronic variant can drive this phenotype. This underscores the importance of considering noncoding regions in patients with characteristic phenotypes but no identified exonic pathogenic variants.

A major contribution of this study is the functional validation of the intronic variant using dual minigene splicing assays. For deep intronic variants and other variants of uncertain significance (VUS), bioinformatic predictions alone are often insufficient for reliable interpretation.[18–20] By consistently confirming aberrant splicing across two vector systems and two cell lines, we provided functional evidence to support reclassification of this variant from "uncertain significance" to "likely pathogenic" under ACMG/AMP guidelines. This highlights the clinical value of functional assays in variant interpretation, directly improving molecular diagnostic yield and providing robust evidence for patient management and genetic counseling.

Nevertheless, this study has certain limitations. First, the splice defect was demonstrated in vitro rather than in patient-derived RNA or protein. This is largely due to the tissue-specific expression of *IMPG2* in the retina/photoreceptors and the practical difficulty of obtaining retinal tissue.[21] Second, this is a single-case report, limiting the generalizability of the conclusions. Validation in larger cohorts, including transcriptome (RNA-seq) and protein-level studies or the use of patient-derived iPSC models, will be important to further elucidate the pathogenic mechanism of the c.909–1659A>G variant.

Looking ahead, combining functional assays with emerging technologies such as RNA-seq and long-read sequencing will be instrumental in clarifying the pathogenicity of noncoding variants. Capasso et al[13] recently demonstrated that targeted long-read cDNA sequencing can identify previously undetected splice-altering events, providing molecular diagnoses for patients with unsolved inherited retinal dystrophies (IRDs). Integrating such molecular evidence with detailed phenotypic data is expected to move variant interpretation from "suspected" to "confirmed," significantly increasing the molecular diagnostic yield and advancing precision medicine and genetic counseling in IRDs.

Data Sharing Statement

Summary-level data supporting the findings of this study are included in the article. Individual-level genomic data cannot be publicly released in accordance with Dove Medical Press data-protection policy. De-identified data may be made available from the corresponding author upon reasonable request and with appropriate ethical approval.

Ethics Statement

This study was conducted in accordance with the Declaration of Helsinki and approved by the Ethics Committee of Boai Hospital of Zhongshan (Approval No. KY-2025-008-05). Written informed consent was obtained from all participants, including permission to publish clinical information, genetic findings, retinal images, and the pedigree. Cross-border processing of de-identified genetic data was conducted in compliance with institutional, national, and GDPR-aligned data-protection regulations.

Acknowledgments

We thank the staff and technicians of the Prenatal Diagnosis Center at Boai Hospital for their invaluable support in data collection and analysis. We are also grateful to colleagues in the participating ophthalmology clinics for assistance with imaging and electrophysiological testing.

Author Contributions

All authors made a significant contribution to the work reported, whether that is in the conception, study design, execution, acquisition of data, analysis and interpretation, or in all these areas; took part in drafting, revising or critically

reviewing the article; gave final approval of the version to be published; have agreed on the journal to which the article has been submitted; and agree to be accountable for all aspects of the work.

Funding

This work was supported by the Zhongshan Science and Technology Bureau (Grant Nos. 2022B1022 and 2023B1042) and the Zhongshan Health Bureau (Grant No. 20241A020003).

Disclosure

The authors declare that they have no competing interests in this work.

References

1. Liu W, Liu S, Li P, et al. Retinitis pigmentosa: progress in molecular pathology and biotherapeutical strategies. *Int J Mol Sci*. 2022;23(9):4883. doi:10.3390/ijms23094883
2. Hartong DT, Berson EL, Dryja TP. Retinitis pigmentosa. *Lancet*. 2006;368(9549):1795–1809. doi:10.1016/S0140-6736(06)69740-7
3. O'Neal TB, Tripathy K, Luther EE. Retinitis Pigmentosa. In: *StatPearls*. Treasure Island (FL): StatPearls Publishing LLC.; 2025.
4. Verbakel SK, Van Huet RAC, Boon CJF, et al. Non-syndromic retinitis pigmentosa. *Prog Retinal Eye Res*. 2018;66:157–186. doi:10.1016/j.preteyeres.2018.03.005
5. Birtel J, Caswell R, De Silva SR, et al. IMPG2-related maculopathy. *Am J Ophthalmol*. 2024;258:32–42. doi:10.1016/j.ajo.2023.10.002
6. Vázquez-Domínguez I, Li CHZ, Fadaie Z, et al. Identification of a complex allele in IMPG2 as a cause of adult-onset vitelliform macular dystrophy. *Invest Ophthalmol Visual Sci*. 2022;63(5):27. doi:10.1167/iovs.63.5.27
7. Britten-Jones AC, Gocuk SA, Goh KL, et al. The diagnostic yield of next generation sequencing in inherited retinal diseases: a systematic review and meta-analysis. *Am J Ophthalmol*. 2023;249:57–73. doi:10.1016/j.ajo.2022.12.027
8. Iancu IF, Avila-Fernandez A, Arteche A, et al. Prioritizing variants of uncertain significance for reclassification using a rule-based algorithm in inherited retinal dystrophies. *NPJ Genom Med*. 2021;6(1):18. doi:10.1038/s41525-021-00182-z
9. Fernández-Suárez E, González-del Pozo M, Méndez-Vidal C, et al. New genetic diagnoses for inherited retinal dystrophies by integrating splicing tools into NGS pipelines. *NPJ Genom Med*. 2025;10(1):52. doi:10.1038/s41525-025-00500-9
10. Hussain HMJ, Wang M, Huang A, et al. Novel pathogenic mutations identified from whole-genome sequencing in unsolved cases of patients affected with inherited retinal diseases. *Genes*. 2023;14(2):447. doi:10.3390/genes14020447
11. Brlek P, Bulić L, Bračić M, et al. Implementing Whole Genome Sequencing (WGS) in clinical practice: advantages, challenges, and future perspectives. *Cells*. 2024;13(6):504. doi:10.3390/cells13060504
12. Walker LC, de la Hoya M, Wiggins GA, et al. Using the ACMG/AMP framework to capture evidence related to predicted and observed impact on splicing: recommendations from the ClinGen SVI Splicing Subgroup. *Am J Hum Genet*. 2023;110(7):1046–1067. doi:10.1016/j.ajhg.2023.06.002
13. Capasso D, Zeuli R, Arno G, et al. Targeted long-read cDNA sequencing reveals novel splice-altering pathogenic variants causing retinal dystrophies. *HGG Adv*. 2025;6(3):100442. doi:10.1016/j.xhgg.2025.100442
14. Richards S, Aziz N, Bale S, et al. Standards and guidelines for the interpretation of sequence variants: a joint consensus recommendation of the American College of Medical Genetics and Genomics and the Association for Molecular Pathology. *Genet Med*. 2015;17(5):405–423. doi:10.1038/gim.2015.30
15. Yuan M, Chatterjee S, Leys M, et al. Prevalence of IMPG1 and IMPG2 mutations leading to retinitis pigmentosa or vitelliform macular dystrophy in a cohort of patients with inherited retinal dystrophies. *Genes*. 2025;16(1):43. doi:10.3390/genes16010043
16. Van Huet RAC, Collin RWJ, Siemiatkowska AM, et al. IMPG2-associated retinitis pigmentosa displays relatively early macular involvement. *Invest Ophthalmol Visual Sci*. 2014;55(6):3939–3953. doi:10.1167/iovs.14-14129
17. Ribarich N, Rivolta MC, Sacconi R, et al. Novel IMPG2 variant causing adult macular vitelliform dystrophy: a case report. *Eur J Ophthalmol*. 2024;34(2):Np1–np4. doi:10.1177/11206721231199850
18. Maggi J, Koller S, Feil S, et al. Limited added diagnostic value of whole genome sequencing in genetic testing of inherited retinal diseases in a swiss patient cohort. *Int J Mol Sci*. 2024;25(12):6540. doi:10.3390/ijms25126540
19. McInnes G, Sharo AG, Koleske ML, et al. Opportunities and challenges for the computational interpretation of rare variation in clinically important genes. *Am J Hum Genet*. 2021;108(4):535–548. doi:10.1016/j.ajhg.2021.03.003
20. Soens ZT, Branch J, Wu S, et al. Leveraging splice-affecting variant predictors and a minigene validation system to identify Mendelian disease-causing variants among exon-captured variants of uncertain significance. *Hum Mutat*. 2017;38(11):1521–1533. doi:10.1002/humu.23294
21. Castellini ME, Spagnolli G, Poggi L, et al. Identification of the zebrafish homologues of IMPG2, a retinal proteoglycan. *Cell Tissue Res*. 2023;394(1):93–105. doi:10.1007/s00441-023-03808-z